American Mineralogist, Volume 73, pages 358–364, 1988

Crystal structure at 25 and 700 °C of magnesiochloritoid from a high-pressure assemblage (Monte Rosa)

GABRIELLA IVALDI
Dipartimento di Scienze della Terra dell'Università, Via S. Massimo 24, 10123 Torino, Italy
MICHELE CATTI
Dipartimento di Chimica Fisica ed Elettrochimica dell'Università, Via Golgi 19, 20133 Milano, Italy
GIOVANNI FERRARIS
Dipartimento di Scienze della Terra dell'Università, Via S. Massimo 24, 10123 Torino, Italy

ABSTRACT

Sets of 2508 and 1556 independent X-ray diffraction data were collected at 25 and 700 °C, respectively, from magnesiochloritoid of a high-pressure assemblage (Monte Rosa, Western Alps). Lattice parameters were measured at several temperatures, and the following values for the principal coefficients of thermal expansion were obtained: 0.77, 1.03, and 1.14 × 10^{-5} K^{-1}. Values at 25 and 700 °C were a = 9.460(1), b = 5.471(1), c = 18.182(2) Å, β = 101.4(1)°; and a = 9.515(3), b = 5.516(2), c = 18.300(7) Å, β = 101.3(3)°, respectively; space group $C2/c$.

The least-squares refinements of the crystal structures at 25 and 700 °C, with composition $(Mg_{0.65}Fe_{0.35})_2Al_4O_2(SiO_4)_2(OH)_4$, converged to R = 0.032 and 0.038. Mean coefficients of thermal expansion for coordination polyhedra are 1, 11, and 13 × 10^{-6} K^{-1} for Si, Al, and (Mg,Fe), respectively. Bond lengths and angles at 25 and 700 °C show that the loss of protons must be simultaneous with the sudden breakdown of the structure at around 750 °C, both in air and in N_2. According to coordination-octahedra size and bond-valence balance, the chloritoid structure should accommodate Fe better than Mg.

INTRODUCTION

Extensive studies have been performed in the last fifteen years on the high-temperature crystal chemistry of rock-forming silicates (Hazen and Finger, 1982). Minerals with OH groups seem to be particularly interesting in this respect, as they undergo thermal dehydration processes that can be preceded by certain structural changes. As a contribution to this field of research, chloritoid was considered, and the structural changes it undergoes at high temperature were investigated.

Chloritoid is a common mineral of high-pressure, low- and intermediate-grade metamorphism; its crystal structure shares features of both nesosilicates (all SiO_4 groups are isolated) and layered silicates. Layers of tetrahedra are connected by two different octahedral layers: (1) a trioctahedral layer with a 1:1 ratio between quite regular (M1A) and strongly distorted (M1B) octahedra and (2) a second layer of quite regular octahedral sites three-quarters filled (M2A and M2B). Owing to this layered structural character, polytypism occurs in chloritoid and has been studied by high-resolution electron microscopy (Jefferson and Thomas, 1978). The two polytypes commonly known are monoclinic and triclinic; the crystal structures were solved and refined both for the former (Harrison and Brindley, 1957; Hanscom, 1975) and the latter (Hanscom, 1980) on samples close to the Fe end member (chloritoid sensu stricto).

Recently Chopin and Monié (1984) described a phengite + talc + chloritoid + chlorite + kyanite + quartz high-pressure assemblage in metapelitic rocks from Monte Rosa (Western Alps) bearing the most magnesian chloritoid (magnesiochloritoid) ever reported. These authors, on the basis of experimental evidence, attributed an important role to chloritoid composition as a barometric indicator in high-grade blueschists; in particular, they estimated that conditions of metamorphism for the assemblage were about 16 kbar and 500 °C. A sample of this chloritoid, kindly provided by C. Chopin, was used for the present study.

The name magnesiochloritoid has been approved by the IMA Commission on New Minerals and Mineral Names by voting in contraposition with the name sismondite. The Commission has recommended to discard the name sismondine (sismondite), which has been used for members of the chloritoid series. Detailed mineralogical data will be published elsewhere.

EXPERIMENTAL DETAILS

All work was performed on pale-green single crystals with irregular shape and dimensions ranging from 0.1 to 0.4 mm; their

0003–004X/88/0304–0358$02.00

TABLE 1. Lattice constants of magnesiochloritoid measured on four single crystals at different temperatures

25 °C	300 °C	500 °C	600 °C	700 °C	750 °C
		a (Å)			
9.456(2)	9.487(3)	9.511(4)	9.516(3)	9.59(2)	
9.461(1)	9.480(2)		9.508(4)	9.512(4)	
9.464(1)	9.489(2)	9.508(2)	9.518(3)	9.527(3)	9.528(3)
9.465(2)*		9.504(3)*	9.513(3)*	9.521(7)*	
		b (Å)			
5.470(1)	5.486(2)	5.498(2)	5.505(2)	5.51(1)	
5.4716(8)	5.490(1)		5.510(2)	5.517(3)	
5.4743(8)	5.490(1)	5.500(1)	5.508(2)	5.512(2)	5.512(2)
5.472(1)*		5.492(2)*	5.499(2)*	5.502(4)*	
		c (Å)			
18.174(2)	18.216(8)	18.249(9)	18.258(8)	18.11(6)	
18.184(3)	18.224(5)		18.275(8)	18.296(9)	
18.191(3)	18.235(4)	18.265(5)	18.286(6)	18.306(7)	18.316(6)
18.195(4)*		18.258(6)*	18.273(6)*	18.30(1)*	
		β (°)			
101.41(2)	101.33(3)	101.29(4)	101.28(3)	102.6(2)	
101.41(1)	101.33(2)		101.27(3)	101.24(4)	
101.39(1)	101.35(1)	101.32(2)	101.32(2)	101.30(3)	101.27(2)
101.50(2)*		101.38(2)*	101.35(2)*	101.31(6)*	
		V (Å^3)			
921.4(3)	929.6(6)	935.8(7)	937.9(6)	934(4)	
922.7(2)	929.9(4)		938.9(6)	941.7(8)	
923.9(2)	931.3(3)	936.6(4)	940.1(5)	942.7(5)	943.4(5)
923.5(3)*		934.2(5)*	937.1(5)*	940(1)*	

* Runs in air flow; other runs in N_2.

chemical composition was checked by WDS microprobe analysis and proved to be very similar to the middle of the range given by Chopin and Monié (1984). A Nicolet R3 four-circle diffractometer, with Mo$K\alpha$ radiation and graphite monochromator, was used for the X-ray study, with an A.E.T. thermal attachment (Argoud and Capponi, 1984); the high temperature (up to 1000 °C) is attained by blowing a stream of hot gas on the crystal. Crystals were fixed to fibers of quartz glass by GA-100 high-temperature cement. All samples examined at room temperature were found to correspond to the monoclinic polymorph of chloritoid.

Four different crystals were analyzed with the same thermal cycle: the temperature was raised to 800 °C in steps of thermal stabilization lasting ≥3 h at 300, 500, 600, and 700 °C; at the end of each step, 24 reflections with $50° < 2\theta < 70°$ were centered and their angular values refined so as to determine the unit-cell parameters (Table 1). Above 750 °C, dehydration occurred suddenly with destruction of the crystal. The lattice parameters could still be determined at 725 and 750 °C, but after staying at the latter temperature for 12 h, the crystal did not diffract X-rays. A flow of hot N_2 was used in three runs, and hot air in the fourth one. On cooling, the lattice parameters of those crystals that did not decompose returned to the values found during the heating cycle, for a given temperature.

The same crystal, with dimensions 0.30 × 0.20 × 0,09 mm^3, was used for intensity-data collection at two temperatures: 25 and 700 °C. At 25 °C the following cell parameters were obtained: $a = 9.460(1)$, $b = 5.471(1)$, $c = 18.182(2)$ Å, $\beta = 101.4(1)°$, $V = 922.6$ Å^3, Z = 4, space group $C2/c$; the intensities of 6410 reflections ($2\theta \leq 80°$), belonging to two centrosymmetrical sets, were measured by the $\omega/2\theta$ scan method (scan width = 2°, background time to scan time ratio = 0.5, scan speed variable between 2.5 and 29.3 deg · min^{-1} with interpolation for intensities ranging from 250 to 2500 counts per second). An empirical absorption correction, based on psi scans of three high-chi reflections with different 2θ (North et al., 1968), was applied, and the transmission coefficient ranged from 0.83 to 1.0. After averaging the equivalent reflections, a unique set of 2508 observed data [$I > 4\sigma(I)$] was obtained (merging R factor = 0.006) for least-squares refinement of the monoclinic crystal structure, starting from the parameters given by Hanscom (1975). The RFINE (Finger and Prince, 1975) and SHELX (Sheldrick, 1981) programs were used. Convergence was attained at $R = 0.053$ for isotropic and $R = 0.032$ for anisotropic thermal factors, respectively. Only one of the two independent H atoms was located with certainty on a difference Fourier map.

Refinement of the site occupancy with RFINE, without chemical constraints, showed only Mg ⇌ Fe substitution, in the M1B site, leading to the formula $(Mg_{0.65}Fe_{0.35})_2Al_4O_2(SiO_4)_2(OH)_4$ (formula weight = 462.83, $d_{calc} = 3.332$ g/cm^3). The results of the refinement are in agreement with the microprobe analysis of the same crystal used for X-ray intensity collection. The average of six measurements (standards: kaersutite, ardennite, celestine) gave SiO_2 27.37, Al_2O_3 44.18, FeO 10.32, MgO 12.14%, and traces of Ti, Sr, Ca, and Mn. The maximum variation was for FeO (9.81–11.02%); this variation is correlated inversely with that of MgO. On the basis of 12 oxygen atoms for the anhydrous residue, the atomic composition $Mg_{1.36}Fe_{0.65}Al_{3.92}Si_{2.06}O_{12}$ is obtained.

At 700 °C [$a = 9.515(3)$, $b = 5.516(2)$, $c = 18.300(7)$ Å, $\beta = 101.3(3)°$, $V = 942.0$ Å^3] a set of 1556 reflections ($2\theta \leq 50°$) was collected, with the same experimental conditions as at room temperature, except for the limitation $-90° < \chi < 75°$ required by the presence of the heating attachment. These limitations prevented measurements for application of the empirical absorption correction. The least-squares refinement, based on 1201 independent reflections with $I > 4\sigma(I)$, converged to $R = 0.065$ and to $R = 0.038$ for isotropic and anisotropic temperature pa-

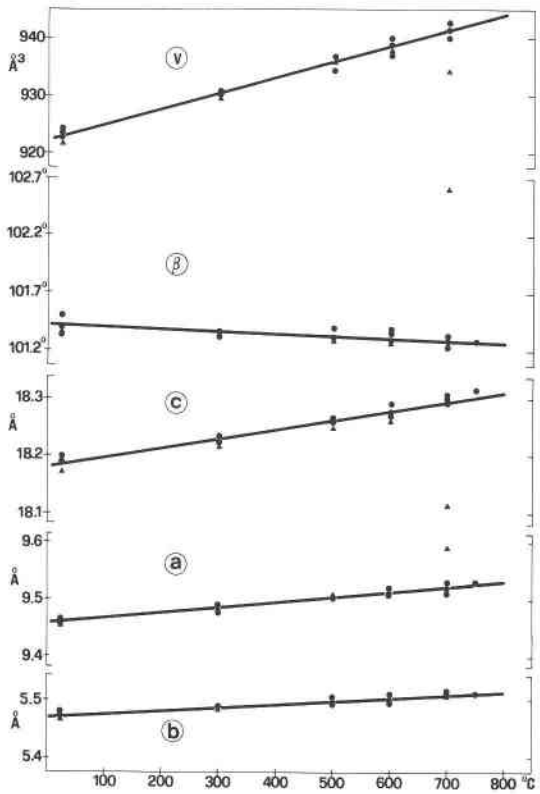

Fig. 1. Lattice parameters of magnesiochloritoid at various temperatures; values and esd's in Table 1. Coefficients for regression lines are given in Table 3. Triangles show values of run 1.

rameters, respectively. Final atomic fractional coordinates are reported in Table 2, for the refinements at both temperatures.[1]

Discussion

Thermal study

According to published TGA and DTA analyses (Bachmann, 1956; Chen, 1963; Fransolet, 1978; van der Plas et al., 1958; Puga, 1970) chloritoid should dehydrate continuously between 400 and 800 °C, depending on chemical composition and physical conditions. A major endothermic effect close to 800 °C is, however, always present in DTA curves. In particular, our observed dehydration temperature at 750 °C may be accounted for because the transformation kinetics are expected to be slower for single crystals than for powder samples. Figure 1 shows the changes in lattice parameters with increasing temperature in both N_2 and air. The behavior observed in run 1 (N_2 atmosphere) is quite different from that of all other runs: after increasing regularly with linear dependence on temperature up to 500 °C, the unit-cell volume begins to deviate negatively from linearity at 600 °C and contracts suddenly at 700 °C, as a consequence of a sharp drop in the c parameter and increase of the β angle below and above their room-temperature values, respectively. In all other runs a quite linear behavior with temperature was obtained, for both volume and lattice parameters until decomposition of the crystals. It should be remarked that at 25 °C the crystal of run 1 showed a and c values significantly smaller than those of the other crystals. Higher esd's at 700 °C clearly indicate that a structure transformation has already set in for this crystal (Table 1).

The first run could give evidence of formation of an intermediate phase before the breakdown of the structure, by small shrinking of the interlayer distance probably due to a loss of water. Unfortunately, that crystal decomposed at higher temperature and was no longer available for a structural study. As such shrinkage of the unit cell did not occur in the other runs performed with the same thermal cycle, the corresponding structure transformation is likely to depend on very subtle kinetic and experimental conditions. The described phenomenon could be related to a splitting (650 and 765 °C) of the major endothermic effect reported by Puga (1970) for a Mg-rich chloritoid; the same author found the usual single peak (766 °C) for Fe-rich chloritoid. On the other hand, in the other runs, no differences in behavior related to the use of air rather than N_2 for heating could be detected.

Linear regressions were carried out for all lattice pa-

TABLE 2. Atomic fractional coordinates and equivalent isotropic temperature factors (Å²) of magnesiochloritoid

	x	y	z	B_{eq}
Al(1A)	¼	¼	0	0.418(8)
	¼	¼	0	1.44(3)
Al(2A)	0	0.4025(1)	¼	0.340(8)
	0	0.4028(3)	¼	1.22(3)
(Mg,Fe)(1B)	0.08397(4)	0.74576(8)	0.00088(2)	0.553(8)
	0.08411(9)	0.7468(2)	0.00070(6)	2.03(2)
Al(2B)	0.24994(6)	0.65365(9)	0.24886(3)	0.347(8)
	0.2498(1)	0.6537(2)	0.24871(7)	1.24(2)
Si	0.46403(4)	0.40298(8)	0.15595(2)	0.268(8)
	0.46414(9)	0.4026(2)	0.15604(5)	0.97(2)
O(1A)	0.1146(1)	0.3927(2)	0.05294(6)	0.58(2)
	0.1147(3)	0.3922(5)	0.0531(1)	1.78(6)
O(1B)	0.2646(1)	0.9447(2)	0.05001(6)	0.55(2)
	0.2640(3)	0.9456(5)	0.0500(1)	1.73(6)
O(1C)	0.4267(1)	0.3977(2)	0.06359(6)	0.49(2)
	0.4270(3)	0.3976(5)	0.0642(1)	1.56(6)
O(2A)	0.3945(1)	0.1589(2)	0.18819(6)	0.39(2)
	0.3949(3)	0.1601(4)	0.1880(1)	1.29(6)
O(2B)	0.3949(1)	0.6479(2)	0.18730(6)	0.39(2)
	0.3949(3)	0.6465(4)	0.1868(1)	1.28(6)
O(2C)	0.1393(1)	0.9037(2)	0.18702(6)	0.39(2)
	0.1385(2)	0.9037(5)	0.1863(1)	1.30(5)
O(2D)	0.1485(1)	0.4016(2)	0.20164(6)	0.32(2)
	0.1493(2)	0.4016(4)	0.2028(1)	1.05(5)
H(1A)*	0.137	0.404	0.112	

Note: Estimated standard deviations are in parentheses. Upper values are at 25 °C; lower ones are at 700 °C.
* At 25 °C.

[1] A copy of structure factors and anisotropic thermal parameters may be ordered as Document AM-88-370 from the Business Office, Mineralogical Society of America, 1625 I Street, N.W., Suite 414, Washington, D.C. 20006, U.S.A. Please remit $5.00 in advance for the microfiche.

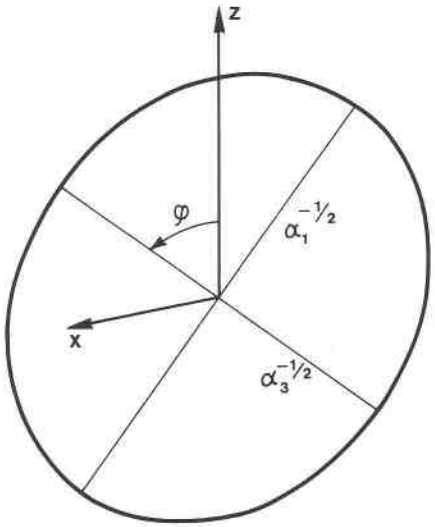

Fig. 2. Ellipsoid of inverse square-root thermal expansion, calculated from linear-regression expansivities of Table 3.

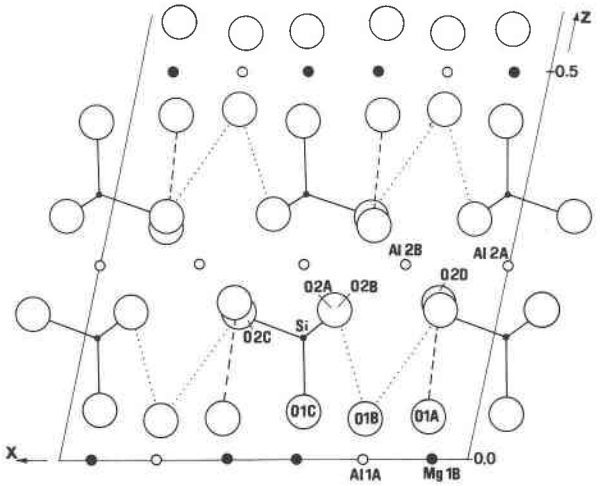

Fig. 3. Projection of half-unit cell of the magnesiochloritoid structure onto (010). Short contacts involving hydroxyls O(1A) and O(1B) are shown.

rameters as a function of temperature between 25 and 700 °C (17 points), excluding the values measured in the first run at 700 °C. Results, including correlation coefficients, and coefficients of thermal expansion are reported in Table 3; the interpolation straight lines are shown in Figure 1. The principal coefficients of thermal expansion were calculated from data of Table 3, yielding $\alpha_1 = 0.77$, $\alpha_2 = 1.03$, $\alpha_3 = 1.14 \times 10^{-5}$ K^{-1}; the α_2 principal axis is parallel to the y axis and the angle between α_3 and the z axis, φ is 55°. In Figure 2 the (010) section of the ellipsoid with semi-axis equal to $\alpha_1^{-1/2}$, $\alpha_2^{-1/2}$, $\alpha_3^{-1/2}$ is shown; the thermal expansion coefficient along a particular crystallographic direction is given by the inverse of the corresponding squared radius. In order to test possible deviations from linearity of the temperature dependence of lattice constants in a single expansion experiment, the parameters of thermal expansion ellipsoids were calculated from unit-cell data of run 3 (Table 1), where the highest temperature of 750 °C was attained, and are reported in Table 4. In case of linearity, all ellipsoids should be equal to one another and to the average one shown in Figure 2; the differences observed are slightly larger than the esd's, indicating that the linear approximation is reasonable. However, a systematic decrease of the φ angle and an increase of the expansion anisotropy are noticed above 600 °C. This would suggest that, within the limits of data significance, the thermal-expansion behavior could signal the approaching dehydration: the expansion tends to become largest between the structural layers in order to facilitate the subsequent loss of water.

Chloritoid crystal chemistry and structure stability

A general view of the structure of monoclinic chloritoid is given in Figure 3, where the sequence of (001) layers of coordination octahedra separated by isolated SiO_4 groups is shown.

Bond distances between cations and oxygen atoms are reported in Table 5 for both structure refinements at 25 and 700 °C. By comparing room-temperature results with those obtained by Hanscom (1975) on a sample close to the Fe end-member chloritoid, no substantial differences can be detected even in sites 1A and 1B, where cation occupancy is quite different in the two samples. The average cation–oxygen bond lengths of the previous study are 1.643, 1.896, 1.896, 1.935, and 2.163 Å for Si, Al2A, Al2B, Al1A, and (Mg,Fe)1B, respectively. By also taking into account the polyhedral dimensions found for the triclinic polymorph (Hanscom, 1980), it appears that the

TABLE 3. Temperature dependence of lattice parameters

	p_0	k (× 10^5)	r	α (× 10^6)
a	9.460(2) Å	9.0(5) Å·K^{-1}	0.98	9.5(5) K^{-1}
b	5.471(2) Å	5.65(40) Å·K^{-1}	0.96	10.3(7) K^{-1}
c	18.179(4) Å	16.2(9) Å·K^{-1}	0.96	8.9(5) K^{-1}
β	101.42(2) deg	−20(4) deg·K^{-1}	0.99	2.0(4) K^{-1}
V	922.1 Å^3	2734(100) Å^3·K^{-1}	0.99	30(1) K^{-1}

Note: Regression coefficients from linear analysis of temperature dependence of lattice parameters, $p = kT + p_0$, correlation coefficient (r), and coefficients of thermal expansion (α) between 25 and 700 °C for magnesiochloritoid.

TABLE 4. Lengths of principal axes of thermal-expansion ellipsoids at different temperatures

	300 °C	500 °C	600 °C	700 °C	750 °C
α_1 (K^{-1})	0.81	0.80	0.86	0.86	0.82 × 10^{-5}
α_2 (K^{-1})	1.04	0.99	1.07	1.02	0.95 × 10^{-5}
α_3 (K^{-1})	1.08	1.09	1.09	1.11	1.12 × 10^{-5}
φ (°)	60	63	61	57	49

Note: Calculated from results of run 3 (Table 1); α_2 is parallel to the y axis, and φ is the angle between α_3 and the z axis. The estimated standard deviations are 3, 5, and 5 × 10^{-7} K^{-1} for α_1, α_2, and α_3, respectively, and 5° for Φ.

TABLE 5. Cation–oxygen bond lengths (Å) and mean coefficients of thermal expansion of coordination polyhedra (K^{-1}) for magnesiochloritoid

	25 °C	700 °C	α
Si–O(1C)	1.647(1)	1.649(3)	
–O(2A)	1.647(1)	1.648(3)	
–O(2B)	1.642(1)	1.645(3)	
–O(2C)	1.642(1)	1.643(2)	
Average	1.645	1.646	1×10^{-6}
Al(1A)–O(1C)	2.005(1)	2.026(2) ×2	
–O(1A)	1.915(1)	1.925(3) ×2	
–O(1B)	1.894(1)	1.905(3) ×2	
Average	1.938	1.952	11×10^{-6}
Al(2A)–O(2D)	1.799(1)	1.801(2) ×2	
–O(2A)	1.945(1)	1.964(3) ×2	
–O(2B)	1.944(1)	1.971(3) ×2	
Average	1.896	1.912	12×10^{-6}
Al(2B)–O(2B)	1.935(1)	1.950(3)	
–O(2D)	1.800(1)	1.800(2)	
–O(2A)	1.949(1)	1.965(3)	
–O(2C)	1.941(1)	1.963(3)	
–O(2C)	1.961(1)	1.988(3)	
–O(2D)	1.798(1)	1.802(2)	
Average	1.897	1.911	11×10^{-6}
(Mg,Fe)(1B)–O(1A)	2.146(1)	2.173(3)	
–O(1B)	2.073(1)	2.084(3)	
–O(1C)	2.208(1)	2.226(3)	
–O(1C)	2.268(1)	2.284(3)	
–O(1A)	2.081(1)	2.099(3)	
–O(1B)	2.126(1)	2.145(3)	
Average	2.150	2.169	13×10^{-6}

TABLE 6. Sums of bond valence for oxygen atoms, without the H contribution

O(1A)	1.169 1.202	O(2A)	1.850 1.850
O(1B)	1.214 1.244	O(2B)	1.878 1.874
O(1C)	1.856 1.886	O(2C)	1.855 1.854
		O(2D)	1.924 1.946

Note: Upper values refer to this work (25 °C); lower values to structural results by Hanscom (1975).

chloritoid structure shows a remarkable rigidity in spite of cation substitution. In particular, the octahedral site 1A, reasonably occupied only by Al^{3+} in magnesiochloritoid, maintains practically the same average Al–O distance reported for the monoclinic Fe-rich chloritoid, where the 1A-site occupancy was (0.92 Al^{3+} + 0.08 Fe^{3+}). The theoretical Al–O value, calculated with Shannon's (1976) ionic radii of Al^{3+} (C.N. 6) and O^{2-} (C.N. 4) is 1.915 Å. The only significant change observed in magnesiochloritoid is the decrease of the average cation–oxygen distance from 2.163 to 2.150 Å in the 1B site, where Mg^{2+} and Fe^{2+} ions are statistically distributed. However, such a decrease is rather small compared to (1) the large change of Fe content between the two structures and (2) the value of 2.121 Å calculated with Shannon's (1976) ionic radii for (0.65 Mg^{2+} + 0.35 Fe^{2+}) and O^{2-} (C.N. 4).

Even if the similarity of their scattering powers does not allow a discrimination between Al and Mg by site-occupancy refinement, an Al ⇌ Mg substitution in the 1B site would be at variance with the large average bond length in this site (2.150 Å). The same substitution in 1A site, instead, could justify the large average bond length of this site (1.938 Å). The chemical analysis, which gives practically four Al atoms in the unit formula, suggests that if such a substitution takes place in the 1A site, it must be very limited.

Hålenius (1982) proposed a linear correlation between the cell volume and the cube of the mean ionic radius of the cations in 1B and 1A sites. The published equation, which did not take into account Mg-rich chloritoids, gives in the present case a value for the volume (914.8 $Å^3$) that is too small with respect to the experimental one (922.6 $Å^3$), confirming the discussed rigidity of the structure.

Published chemical analyses (Deer et al., 1982; Halferdahl, 1961) show that Mg-rich chloritoid tends to have no Fe^{3+} and an Al content of 4 atoms per unit formula, sufficient to fill layer 1 and one site of layer 2. On the other hand, the rigid 1B and 1A sites are too large to accommodate only Mg and Al atoms, respectively. Therefore, as the chloritoid structure appears unlikely to contract when larger cations are deficient in the 1A and 1B sites, the abundance in nature of Fe-rich relative to Mg-rich chloritoids seems to be justified on structural grounds. Thus far, only a few occurrences of magnesiochloritoid have been found, and all are in rocks subjected to high-pressure, low-temperature metamorphism. In other conditions, Chinner and Dixon (1973) have shown that Mg-rich chloritoid is unstable and that the following transformation occurs: (Mg,Fe)-chloritoid + quartz = kyanite + talc + (Fe,Mg)-chloritoid + water.

The greater ease of accommodation of Fe, rather than Mg, in the chloritoid structure seems supported by bond-valence considerations, as well. Calculations according to Brown and Wu's (1976) method, exclusive of the contributions from the H atoms, show (Table 6) that the overall underbonding of the oxygen atoms is lower for Fe-rich (11.86 v.u.) than for Mg-rich chloritoid (11.75 v.u.). In particular, O1C (not affected by hydrogen bonds) and O1A, which are octahedrally coordinated by cations of 1B and 1A sites only, improve their bond-valence sum in the Fe-rich chloritoid.

High-temperature structure

Owing to the rigid connection required by the layered topology, no substantial tilting of coordination polyhedra is present in magnesiochloritoid, and the thermally induced changes in the structure between 25 and 700 °C can be analyzed mainly on the basis of the thermal expansion of polyhedra. This expansion is defined by the formula $\alpha_{T_1,T_2} = [2/(d_1 + d_2)][(d_2 - d_1)/(T_2 - T_1)]$, where d_1 and d_2 are the average cation–oxygen distances within the coordination polyhedron at temperatures T_1 and T_2,

TABLE 7. RMS deviations of M–O bond distances and bond angles

	1	2
Al(1A)	0.048	6.2
	0.053	6.0
Al(2A)	0.069	3.7
	0.079	3.9
Al(2B)	0.070	3.6
	0.079	3.7
(Mg,Fe)(1B)	0.069	11.5
	0.070	11.4

Note: (1) $[\Sigma(d_i - d)^2/6]^{1/2}$ (in Å) and (2) $[\Sigma(\varphi_i - 90°)^2/12]^{1/2}$ (in °) for the cation coordination octahedra at 25 °C (upper values) and 700 °C (lower values) in magnesiochloritoid.

respectively (Table 3). The well-known result that the SiO_4 tetrahedron is not significantly affected by thermal expansion is confirmed here; the dilation of the structure can be ascribed entirely to contributions of the Al and (Mg,Fe) coordination polyhedra, in similar amounts, showing expansivities very close to those of the whole unit cell. Therefore, different parts of the structure expand unequally with temperature, particularly along **c**, and this causes internal strains at the interlayer junctions.

A slightly larger thermal expansion is observed for the (Mg,Fe) than for the Al octahedra. The values of α_{T_1,T_2} reported in the literature for the most important silicates range from 7×10^{-6} K^{-1} (sillimanite, pyrope) to 12×10^{-6} K^{-1} (andalusite), with an average of 9×10^{-6} K^{-1} in the case of Al; from 9×10^{-6} K^{-1} (fluoro-phlogopite) to 17×10^{-6} K^{-1} (phlogopite), with an average of 14×10^{-6} K^{-1} in the case of Mg; and from 10×10^{-6} K^{-1} (hedenbergite) to 24×10^{-6} K^{-1} (orthoferrosilite), with an average of 16×10^{-6} K^{-1} in the case of Fe^{2+} (Hazen and Finger, 1982). Thus we may say that in magnesiochloritoid the Al and (Mg,Fe) octahedra have thermal-expansion coefficients that are close to the largest and lowest values, respectively, observed in other silicates. The 1B octahedron was remarked on above to be fairly large with respect to the high Mg content, so it is not unexpected that its thermal expansion tends to be low with a large expansion of Al polyhedra compensating for it.

The effect of temperature on the regularity of coordination polyhedra of cations M is shown by Table 7, where the root-mean-square deviations from the average are reported for the M–O distances and for the O–M–O angles (excluding the three octahedral angles close to 180°), both at 25 and 700 °C. Distortions of octahedra seem to be observed at high temperature, or even slightly increased in the case of polyhedra belonging to the Al layer, in spite of the well-known tendency of crystal structures toward higher symmetry at higher temperatures. This should be ascribed to the strongly inhomogeneous thermal expansion observed for the magnesiochloritoid structure, which is related to the different expansivities of SiO_4 tetrahedra and metal octahedra, causing strong interlayer strains.

TABLE 8. Distances (Å) of short contacts betwen OH^- ions and oxygen atoms in magnesiochloritoid

	25 °C	700 °C
O(1A)···O(2D)	2.660(2)	2.694(3)
O(1B)···O(2A)	2.824(2)	2.846(4)
O(2B)	3.028(2)	3.053(4)
O(2C)	2.972(2)	2.978(4)

Hydroxyl content and dehydration mechanism

In Table 8 the interatomic distances of O1A and O1B, carrying H atoms according to Hanscom's (1975) results, with possible acceptors of hydrogen bonds, are reported for both room- and high-temperature structures. The H1A atom was located (25 °C) at distances of 1.06 and 1.61 Å from O1A and O2D, respectively, with an O–H···O angle of 171°, thus confirming the formation of a short hydrogen bond. The H atom belonging to O1B could not be identified in the difference maps. A bond-valence calculation, while confirming that O1B must be a hydroxyl, shows no appreciable differences among the possible acceptors O2A, O2B, and O2C, all being similarly underbonded (Table 8).

Distances at high temperature (Table 5), including O···O hydrogen bonds (Table 8), are, apart from thermal expansion, the same as found at 25 °C. Thus H atoms must still be fully attached to O1A and O1B in order to account for the bond valence of these oxygen atoms. According to our results, at least for the present Mg-rich sample, and probably for other chloritoids too, dehydration is a catastrophic event leading to the breakdown of the crystal structure. The dehydration mechanism based on $Fe^{2+} \rightarrow Fe^{3+}$ oxidation and simultaneous deprotonation, suggested by Bachmann (1956), is not supported by the present results. Such a mechanism would at least require a rearrangement of M1B–O distances in order to redistribute the higher valence of Fe^{3+} among the oxygen atoms, particularly the (partially) deprotonated O1A and O1B.

ACKNOWLEDGMENTS

We thank C. Chopin (Paris) for kindly providing the sample of magnesiochloritoid used in this work and B. Lombardo (Torino) for very useful discussions.

REFERENCES CITED

Argoud, R., and Capponi, J.J. (1984) Soufflette à haute température pour l'étude de monocristaux aux rayons X et aux neutrons jusqu' à 1400 K. Journal of Applied Crystallography, 17, 420–425.

Bachmann, H.G. (1956) Dehydration von Chloritoiden. Zeitschrift für Kristallographie, 108, 145–156.

Brown, I.D., and Wu, K.K. (1976) Empirical parameters for calculating cation–oxygen bond valences. Acta Crystallographica, B32, 1957–1959.

Chen, P. (1963) Mineralogy and petrology of the chloritoid rock from Shakatangchi and Laohsichi area, Hualien, Taiwan. Acta Geologica Taiwanica, 10, 11–27.

Chinner, G.A., and Dixon, J.E. (1973) Some high-pressure parageneses of the Allalin gabbro, Valais, Switzerland. Journal of Petrology, 14, 185–202.

Chopin, C., and Monié, P. (1984) A unique magnesiochloritoid-bearing assemblage from the Monte Rosa, Western Alps: Petrologic and ^{40}Ar-^{39}Ar radiometric study. Contributions to Mineralogy and Petrology, 87, 388–398.

Deer, W.A., Howie, R.A., and Zussman, J. (1982) Rock-forming minerals: Vol. 1A, Orthosilicates. Longman, London.

Finger, L.W., and Prince, E. (1975) A system of Fortran IV computer programs for crystal structure computations. U.S. National Bureau of Standards Technical Note 854.

Fransolet, A.M. (1978) Données nouvelles sur l'ottrélite d'Ottré, Belgique. Bulletin de Minéralogie, 101, 548–557.

Hålenius, U. (1982) Monoclinic chloritoid: Calculations of unit cell volumes and densities in the pseudo-ternary system Fe-Ctd–Mn-Ctd–Mg-Ctd. Lithos, 15, 249–251.

Halferdahl, L.B. (1961) Chloritoid: Its composition, X-ray and optical properties, stability, and occurrence. Journal of Petrology, 2, 49–135.

Hanscom, R.H. (1975) Refinement of the crystal structure of monoclinic chloritoid. Acta Crystallographica, B31, 780–784.

——— (1980) The structure of triclinic chloritoid and chloritoid polymorphism. American Mineralogist, 65, 534–539.

Harrison, F.W., and Brindley, G.W. (1957) The crystal structure of chloritoid. Acta Crystallographica, 10, 77–82.

Hazen, R.M., and Finger, L.W. (1982) Comparative crystal chemistry. Wiley, Chichester.

Jefferson, D.A., and Thomas, J.M. (1978) High resolution electron microscopic and X-ray studies of non-random disorder in an unusual layered silicate (chloritoid). Proceedings of the Royal Society of London, A361, 399–411.

North, A.E.T., Phillips, D.C., and Mathews, F.S. (1968) A semiempirical method of absorption correction. Acta Crystallographica, A24, 351–359.

Puga, E. (1970) Tres variedades de cloritoide en Sierra Nevada (Cordilleras Beticas, España). Cuadernos Geologicos (Spain), 1, 65–70.

Shannon, R.D. (1976) Revised effective ionic radii and systematic studies of interatomic distances in halides and chalcogenides. Acta Crystallographica, A32, 751–767.

Sheldrick, G.M. (1981) SHELXTL. An integrated system for solving, refining and displaying crystal structures from diffraction data (3rd revision). University of Göttingen.

van der Plas, L., Hügi, T., Mladeck, M.H., and Niggli, E. (1958) Chloritoid vom Hennensädel südlich Vals (nördliche Aduladecke). Schweizerische Mineralogische und Petrologische Mitteilungen, 38, 237–246.

Manuscript received February 25, 1987
Manuscript accepted September 14, 1987